Supplementary information

Supplementary Figures

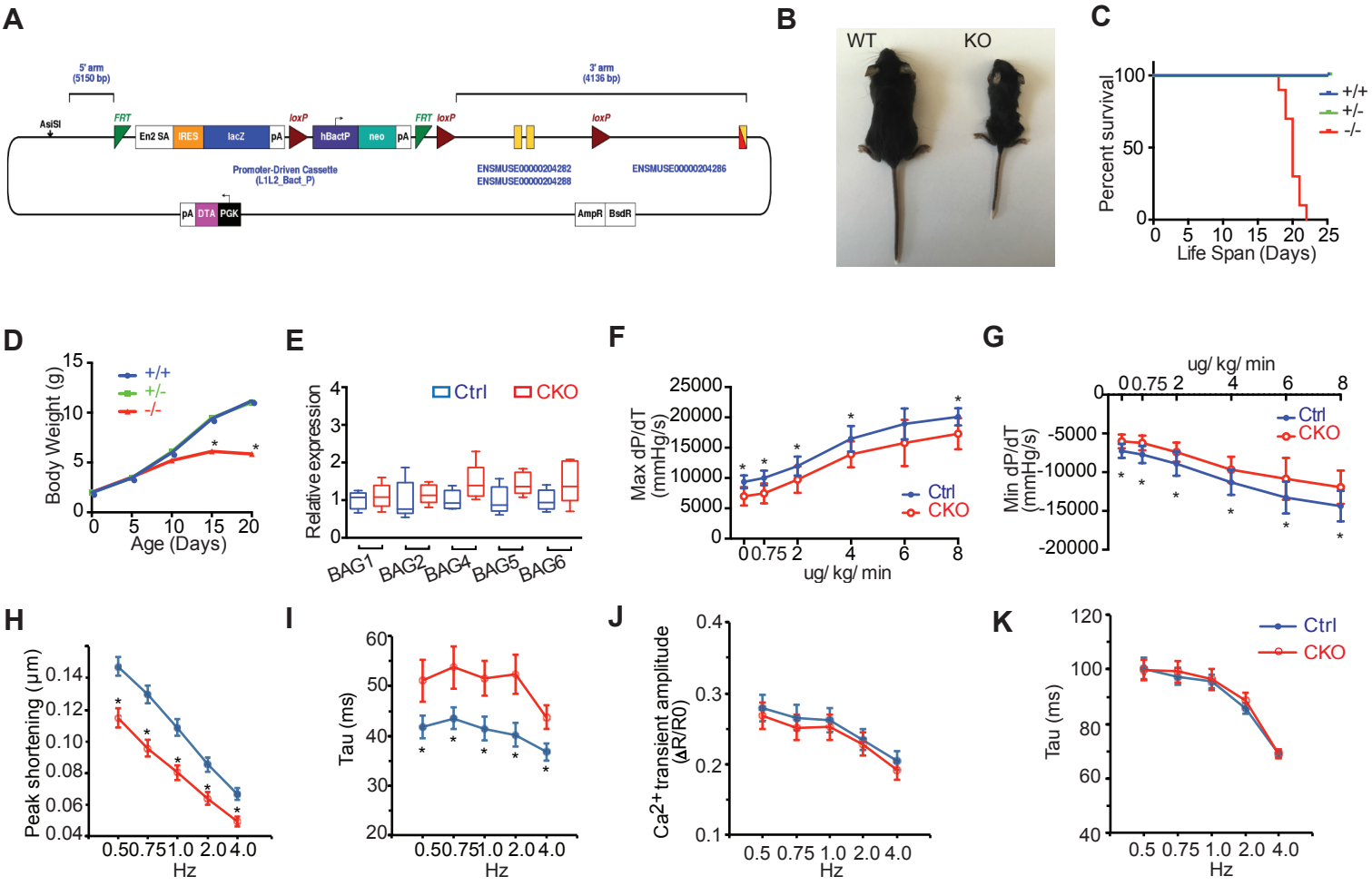

Figure S1. (Relative to Figure 1) BAG3 deficiency leads to DCM and premature death. (A) Targeting strategy for the generation of BAG3 knockout mice. **(B)** Representative image to illustrate significant growth retardation in BAG3 global knockout mice compared with wildtype (WT) littermates at 20 days of age (scale bar: 1 cm). **(C)** Kaplan-Meier survival curves of BAG3 global knockout homozygous (-/-), heterozygous (+/-) and control (+/+) mice. n=10 mice per group. **(D)** Growth curves of BAG3 global knockout homozygous (-/-), heterozygous (+/-) and control (+/+) mice. n=10 mice per group. **(E)** qRT-PCR analysis of BAG1, BAG2, BAG4, BAG5, BAG6 in control (Ctrl) (n=9) and BAG3f/f; α-MHC-Cre positive (CKO) (n=8) mouse hearts at 4 months. Data is normalized to corresponding 18S levels. **(F-G)** Hemodynamic measurements of contractile function in Ctrl (n=7) and BAG3 CKO (n=11) mice in response to increasing levels of the beta 1 adrenergic agonist dobutamine at 10 weeks. **(H-I)** The contractility of adult cardiomyocytes isolated from Ctrl and BAG3 CKO mice were measured using a sarcomere length-detection system. The amplitude of cell contraction was assessed by peak shortening (H), and the rate of cell relaxation was assessed by the time to 63% re-lengthening (Tau) (I). **(J-K)** The amplitude (J) and Tau (K) of Ca2+ transients of Ctrl (blue) and BAG3 CKO (red) cardiomyocytes were measured at 0.5, 0.75, 1.0, 2.0, and 4.0 Hz, respectively. Data are represented as mean ± SEM; *P<0.05 according to 2-tailed Student's t test.

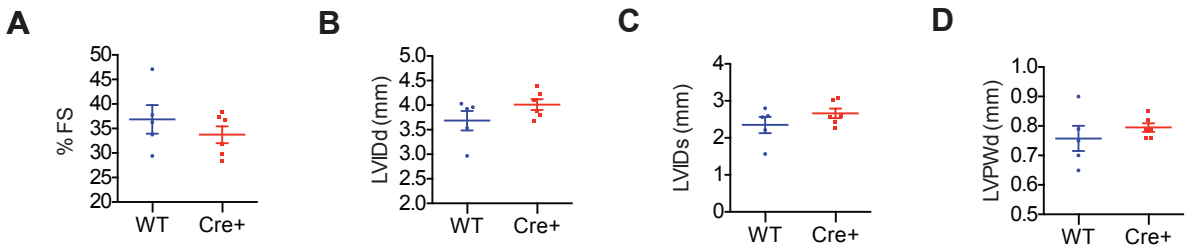

Figure S2. Echocardiographic measurements from wildtype (WT) (n=5) and αMHC-Cre positive (Cre+) (n=6) mice at 10 months. (A) Left ventricle (LV) fractional shortening (FS); **(B-C)** LV internal diameter at end diastole (B) LV internal diameter at and end systole (C). Data are represented as mean ± SEM.

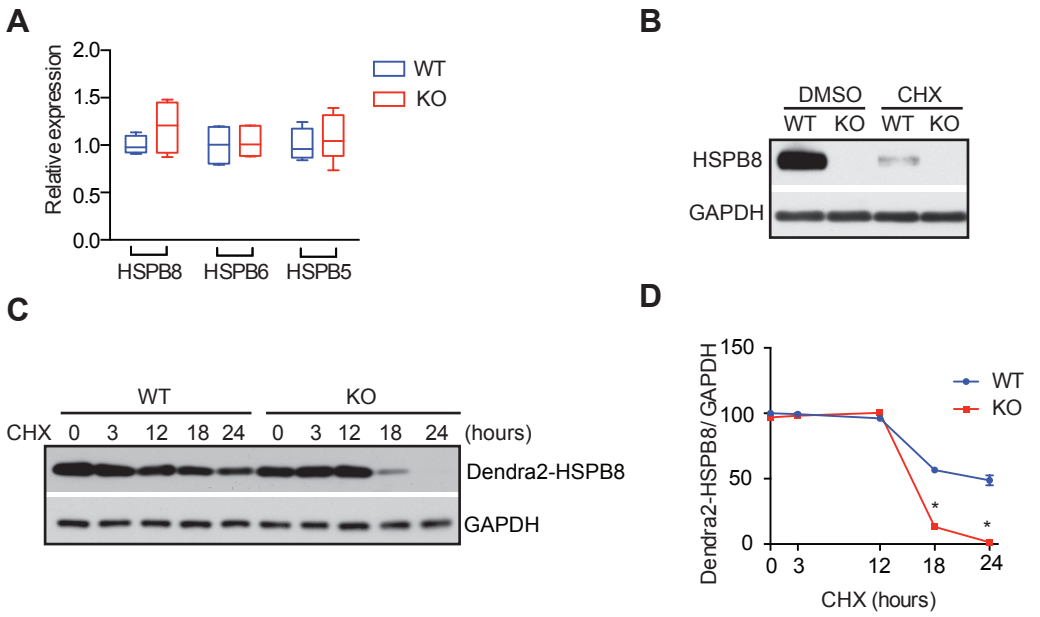

Figure S3. BAG3 deficiency leads to protein instability of sHSPs. (A) qRT-PCR analysis of HSPB8/6/5 in BAG3 global knockout (KO) (n=5) and wildtype (WT) control (n=4) hearts at 2 weeks. Data is normalized to corresponding 18S levels. **(B)** Western blot analysis of HSPB8 in neonatal cardiomyocytes isolated from WT control and BAG3 KO mice treated with cycloheximide (CHX, 10 μg/ml) for 24 hours. DMSO was used as a control. n=3. GAPDH served as a loading control. **(C-D)** Representative western blot (C) and quantification analysis (D) of overexpressed Dendra2-HSPB8 in neonatal cardiomyocytes isolated from WT control and BAG3 KO mice infected with HSPB8 fused with Dendra2 taq overexpressing adenovirus (20 MOI). After 24 hour infection, cardiomyocytes were treated with CHX (10 μg/ml) for 0, 3, 12, 18, 24 hours. GAPDH served as a loading control. Data are represented as mean ± SEM; *P<0.05 according to 2-tailed Student's t test.

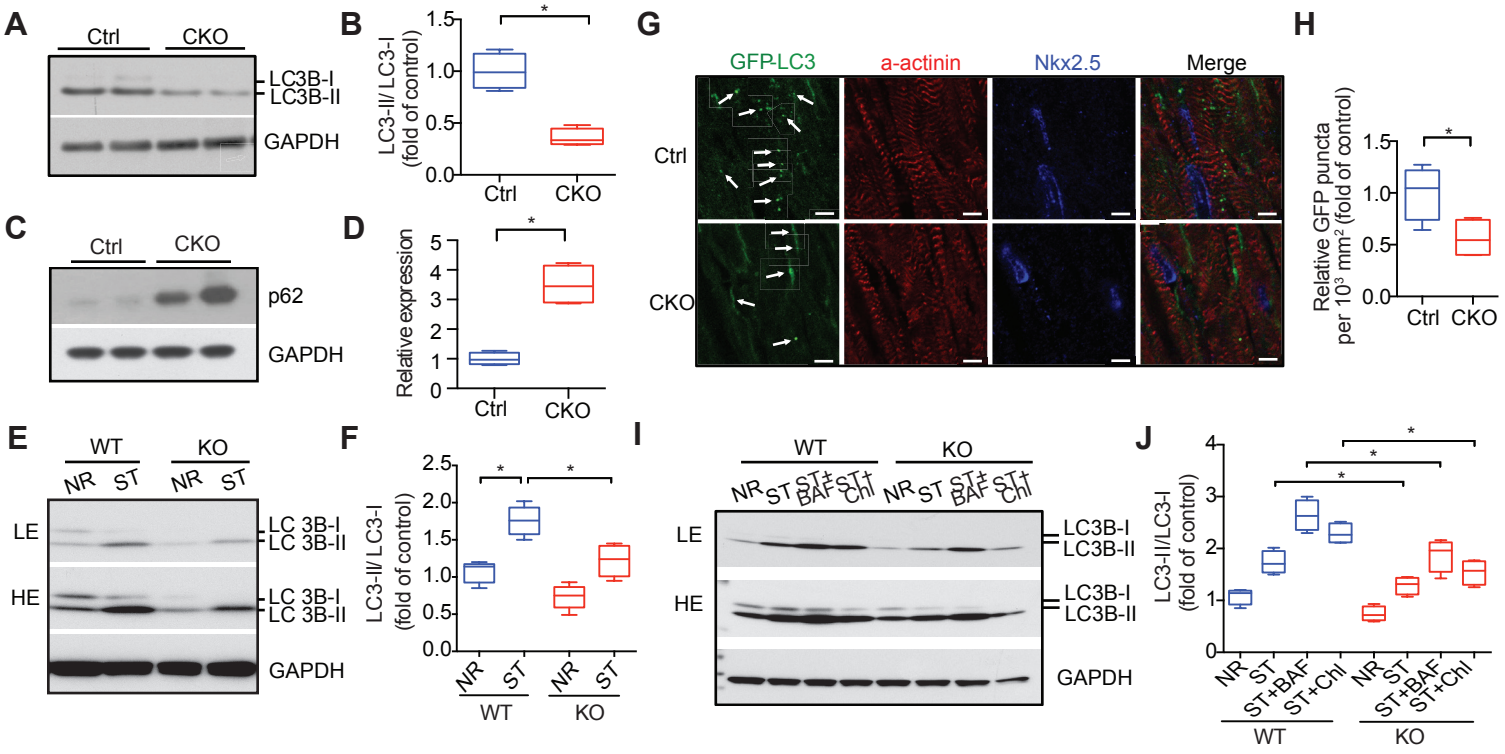

Figure S4. Autophagic flux is suppressed in BAG3 knockout hearts and cardiomyocytes. (A-B) Representative Western blot (A) and quantification analysis (B) of cardiac autophagic flux assessed by the ratio of LC3-II to LC3-I in control (Ctrl) and BAG3f/f; αMHC-Cre positive (CKO) hearts after 18 hour fasting. n=4 mice per group. **(C-D)** Representative Western blot (C) and quantification analysis (D) of p62 protein levels in cardiac tissues from Ctrl and BAG3 CKO mice. n=4 mice per group. **(E-F)** Representative Western blot (E) and quantification analysis (F) for starvation-induced cardiac autophagic flux assessed by the ratio of LC3-II to LC3-I in neonatal cardiomyocytes isolated from wildtype (WT) control and BAG3 knockout (KO) mice. NR: Nutrition rich; ST: starvation 3 hours in glucose and serum deplete medium. n=5. **(G-H)** Representative images (G) and quantification analysis (H) of cardiac tissue sections from Ctrl and BAG3 CKO mice crossed with GFP-LC3 (green) transgenic mice after 18 hour fasting. α-actinin and Nkx2.5 staining were used for labeling cardiomyocytes. n=4 mice per group. **(I-J)** Representative immunoblots (I) and quantification analysis (J) for cardiac autophagic flux assessed by the ratio of LC3-II to LC3-I in neonatal cardiomyocytes isolated from WT and BAG3 KO mice under different treatment conditions for 3 hours. GAPDH served as a loading control. NR: Nutrition rich; ST: starvation in glucose and serum deplete medium; BAF: Bafilomycin A1; Chl: Chloroquine. GAPDH was used as loading control. n=4. Data are represented as mean ± SEM; *P<0.05 according to 2-tailed Student's t test or two way ANOVA.

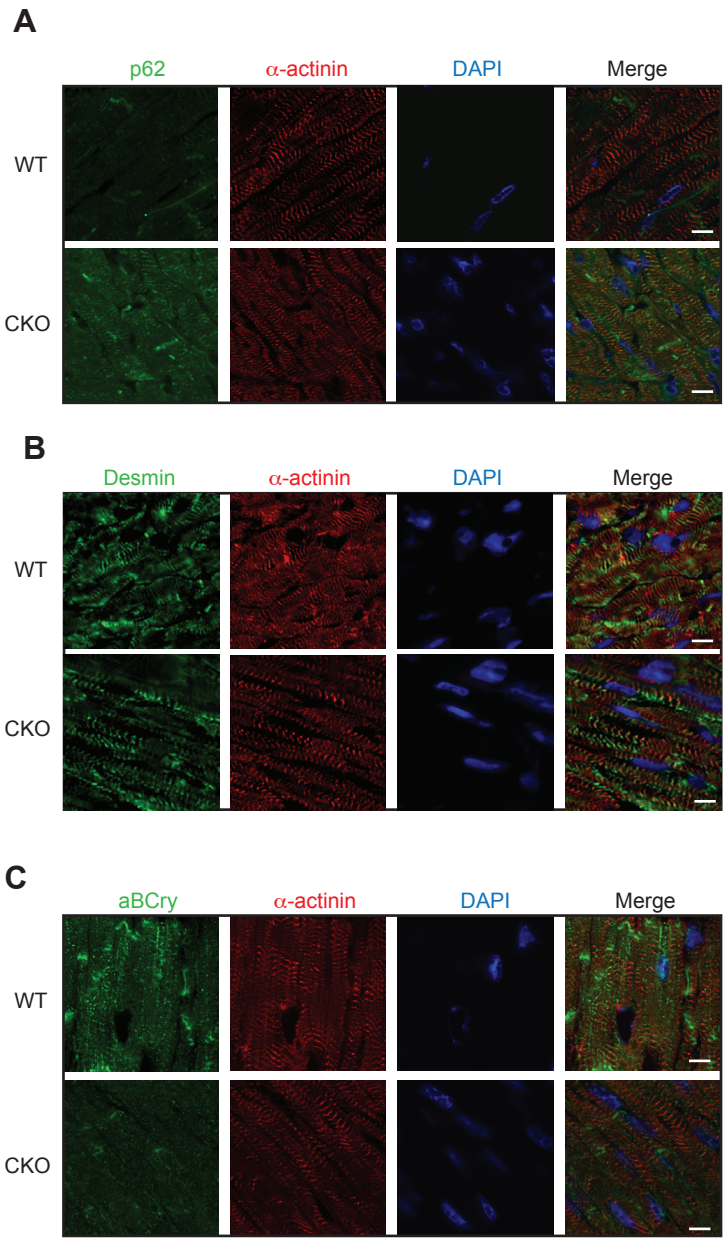

Figure S5. Immunofluorescence analysis of BAG3-related proteins **(A)** p62, **(B)** Desmin,and **(C)** αB-crystalin in myocardium of control (Ctrl) and BAG3f/f; α-MHC-Cre positive (CKO) mice. n=3 mice per group. Scale bars: 5 μm.

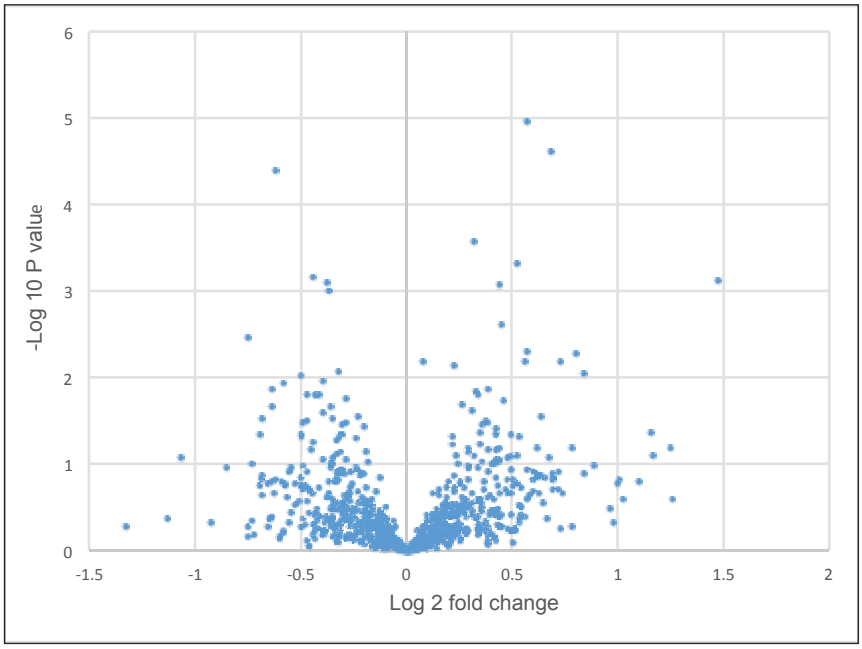

Figure S6. Volcano Plot showing P values (-log10) versus protein quantitation ratio of CKO/Ctrl (log2) of total proteins from iTRAQ analysis of BAG3 CKO and control hearts.

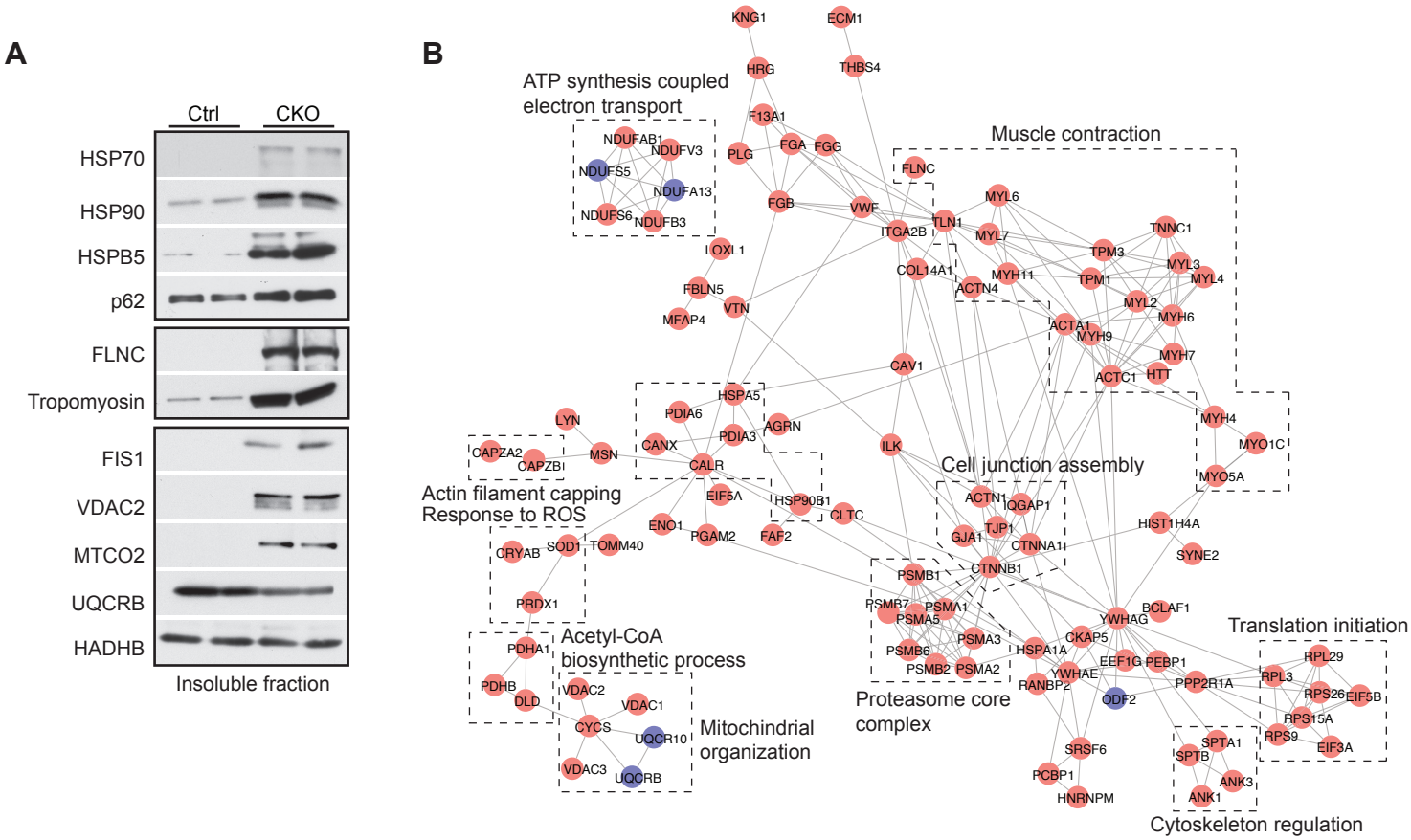

Figure S7. (Relative to Figure 3) BAG3 deficiency leads to increased levels of a subset of insoluble proteins. **(A)** Western blot validation of mass spectrometry analysis of insoluble fraction proteins from Ctrl and CKO mouse hearts. n = 4. Loading control in Figure 3B was used for replicate samples in Figure 7A. **(B)** Network visualization of the highly differentially expressed proteins from insoluble fraction of Ctrl versus CKO mouse hearts. Red nodes represent increased proteins (fold change greater than 3 in CKO/Ctrl). Blue nodes represent decreased proteins (fold change less than 0.5 in CKO/Ctrl). Enriched gene ontology (GO) terms of network modules were defined by DAVID functional annotation tool.

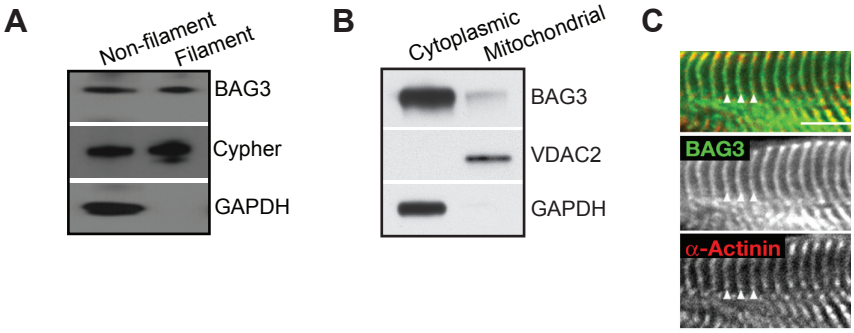

Figure S8. Localization of BAG3 in adult mouse heart. (A) BAG3 is present in both non-filament and filament fractions of total proteins isolated from wildtype adult mouse ventricles. Cypher is a known Z-disk protein. GAPDH was used as a cytosolic protein marker. **(B)** BAG3 is present in both cytoplasmic and mitochondrial fractions of total proteins isolated from wildtype adult mouse ventricles. VDAC2 and GAPDH were used as mitochondrial and cytosolic protein markers, respectively. **(C)** BAG3 (green) colocalizes with α-Actinin (red) at Z-disks (arrowheads) in wildtype mouse heart sections.

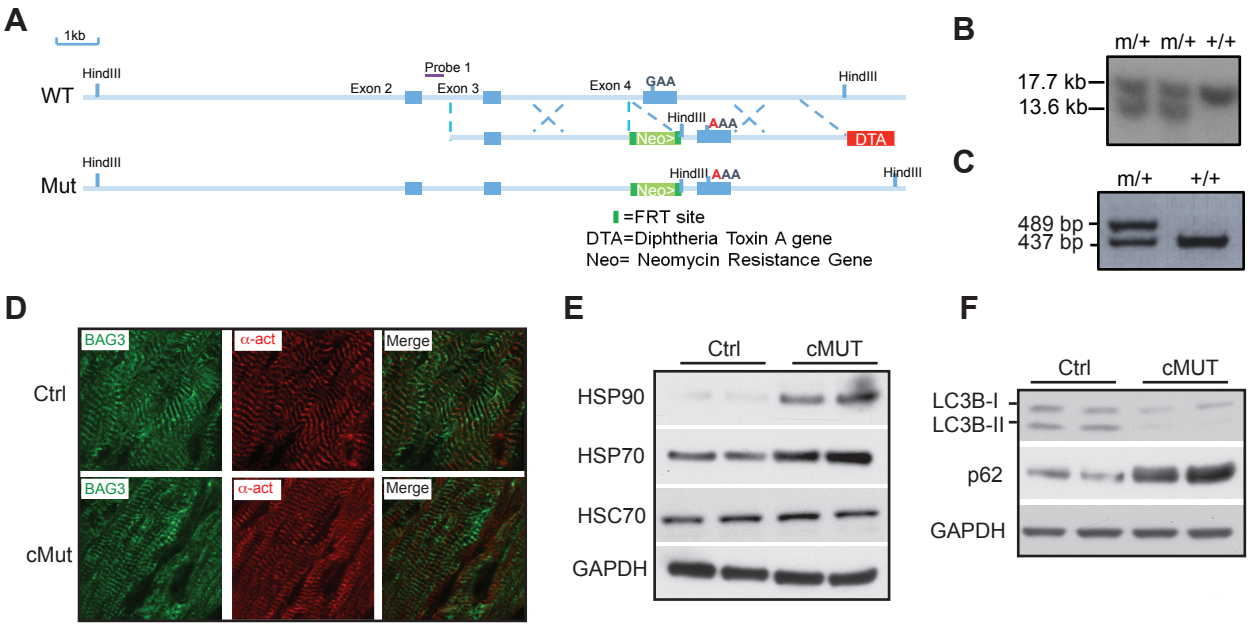

Figure S9. (Relative to Figure 6) E455 amino acid is critical for BAG3 function. (A) Targeting strategy for the generation of E455K knock-in mice. Neo, neomycin resistance gene; DTA, Diphtheria Toxin A chain gene. Green boxes abutted to the Neo gene indicate FRT sites. **(B)** Detection of wildtype (+) and mutant (m) alleles by Southern blot analysis. **(C)** Genotyping of BAG3 E455K mutant mice. **(D)** Immunofluorescence analysis of BAG3 in myocardium of control (Ctrl) and cardiac-specific BAG3 E455K mutant (cMUT) mice. Scale bars: 2 μm. n=3 mice per group. **(E)** Representative Western blot analysis of HSP90, HSP70, HSC70 in cardiac tissues from Ctrl and cMUT mice. n=4 mice per group. **(F)** Representative Western blot analysis of cardiac autophagic flux assessed by the ratio of LC3B-II to LC3B-I in Ctrl and cMUT hearts after 18 hour fasting. GAPDH served as a loading control. n=4 mice per group.

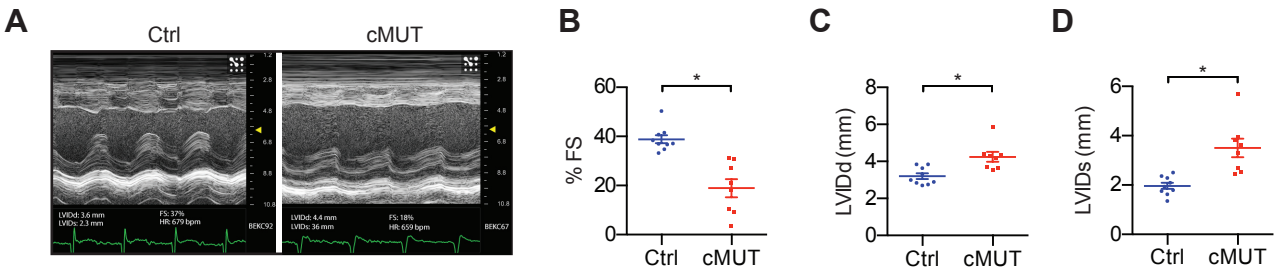

Figure S10. Echocardiographic measurements from cardiac specific BAG3 E455K mutant (cMUT) and control (Ctrl) mice at 6 months. (A) Representative images of echocardiography from Ctrl and cMUT mice at 6 months. **(B-D)** Echocardiographic measurements from Ctrl (n=9) and cMUT (n=8) mice at 6 months of (B) left ventricle (LV) fractional shortening (FS), (C) LV internal diameter at end diastole and (D) LV internal diameter at end systole. Data are represented as mean ± SEM; *P<0.05 according to 2-tailed Student's t test.

Supplemental methods

Aggregate purification and mass spectrometry

Aggregate purification was performed as described previously(1). Briefly, tissue samples were pulverized in a dry-ice-cooled mortar, and suspended in lysis buffer (20-mM HEPES pH 7.4, 0.3-M NaCl, 2 mM MgCl2, 1% NP40 (w/v), and phosphatase/protease inhibitors (Roche, IN, USA)). After centrifugation (5 mins, 2000 x g) to remove debris, organelles and particulates, protein concentration was determined (BCA protein assay kit, Thermo Fisher Scientific, MA, USA). Equal total protein amounts were applied to aggregate purification and analyzed by silver stain. Protein samples were centrifuged at 14,000 g for 15 mins and the supernatants removed. Pellets were suspended in 0.1 M HEPES buffer containing 1% sarcosyl (v/v), 5 mM EDTA, and protease inhibitors, followed by 30 min centrifugation at 100,000 x g. The detergent-insoluble pellet (100,000-g pellet) from different samples was suspended in urea lysis buffer (8 M Urea, 2 M Thiourea, 3% SDS, 75 mM DTT, 0.03% Bromophenol Blue, 0.05 M Tris-HCl, pH 6.8) for gel analysis. For the proteomic study of aggregates, pellets from different samples were dissolved in 8 M urea 50 mM ammonium bicarbonate buffer and sonicated followed by digestion. Briefly, cysteine disulfide bonds were reduced with 5 mM tris (2-carboxyethyl) phosphine (TCEP) at 30°C for 60 mins followed by cysteine alkylation with 15 mM iodoacetamide (IAA) in the dark at room temperature for 30 mins. Following alkylation, urea was diluted to 1 M urea using 50 mM ammonium bicarbonate, and proteins were finally subjected to overnight digestion with MS grade Trypsin/Lys-C mix (Promega, Madison, WI). Digested proteins were finally desalted using a C18 TopTip (PolyLC, Columbia, MD) according to the manufacturer's recommendation), and the organic solvent was removed in a SpeedVac concentrator prior to LC-MS/MS analysis. The functional interaction network among the strongly changed proteins (fold change greater than 3 or less than 0.5 in CKO/control) were constructed based on Wu et al.

2010 (2). Network modules of the strongly changed proteins in CKO/control were clustered by Markov cluster algorithm (MCL) with the granularity parameter set to 2.5. We visualized the networks by Cytoscape (3).

Flag-HA tandem pull-down and mass spectrometry

Neonatal cardiomyocytes were infected with adenoviruses expressing 3Flag-HA-BAG3 or control 3Flag-HA-GFP. After 48 hours of infection, cardiomyocytes were lysed and immunoprecipitated with anti-Flag M2 agarose (Sigma) overnight at 4°C. The beads were washed and eluted. After removal of the Flag-agarose, the eluates were immunoprecipitated with anti-HA agarose (Sigma) at 4°C overnight. HA agarose was washed and then eluted with 8 M urea at room temperature for 10 mins. The immunoprecipitated products were separated on SDS-PAGE gels and analyzed with silver stain (Thermo Fisher Scientific). Resulting bands different from the GPF control group were analyzed by mass spectrometry (MS). For the interacting protein profiling, following immunoprecipitation, proteins were digested directly on-beads. Briefly, proteins bound to the beads were resuspended with 8 M urea, 50 mM ammonium bicarbonate, and cysteine disulfide bonds were reduced with 10 mM tris (2-carboxyethyl)phosphine (TCEP) at 30°C for 60 mins followed by cysteine alkylation with 30 mM iodoacetamide (IAA) in the dark at room temperature for 30 mins. Following alkylation, urea was diluted to 1 M urea using 50 mM ammonium bicarbonate, and proteins were subjected to overnight digestion with MS grade Trypsin/Lys-C mix (Promega, Madison, WI). Finally, beads were pulled down and the solution with peptides collected into a new tube. The beads were then washed once with 50 mM ammonium bicarbonate to increase peptide recovery. The digested proteins were desalted using a C18 TopTip (PolyLC, Columbia, MD), and the organic solvent was removed in a SpeedVac concentrator prior to LC-MS/MS analysis. The cytoplasmic proteins that were found only in BAG3 overexpressing

cells, or at least 20-fold enriched compared to GFP group were selected as BAG3 potential binding partners. The Gene Ontology Enrichment Analysis (GOEA) was performed by Toppgene platform (https://toppgene.cchmc.org/)(4). The interactome network among the BAG3 potential binding partners were constructed based on Wu et al. 2010 (2). Network modules of the strongly changed proteins in CKO/control were clustered by Markov cluster algorithm (MCL) with the granularity parameter set to 2.5. The network was visualized by Cytoscape (3).

2DLC-MS/MS analysis and data analysis

Dried samples were reconstituted in 100 mM ammonium formate pH ~10 and analyzed by 2DLC-MS/MS using a 2D nanoACQUITY Ultra Performance Liquid Chromatography (UPLC) system (Waters corp., Milford, MA) coupled to a Q-Exactive Plus mass spectrometer (Thermo Fisher Scientific). Peptides were loaded onto the first dimension column, XBridge BEH130 C_{18} NanoEase (300 µm x 50 mm, 5 µm) equilibrated with solvent A (20 mM ammonium formate pH 10, first dimension pump) at 2 µL/min. The first fraction was eluted from the first dimension column at 17% of solvent B (100% acetonitrile) for 4 mins and transferred to the second dimension Symmetry C18 trap column 0.180 x 20 mm (Waters corp., Milford, MA) using a 1:10 dilution with 99.9% second dimensional pump solvent A (0.1% formic acid in water) at 20 µL/min. Peptides were then eluted from the trap column and resolved on the analytical C_{18} BEH130 PicoChip column 0.075 x 100 mm, 1.7 µm particles (NewObjective, MA) at low pH by increasing the composition of solvent B (100% acetonitrile) from 2 to 26% over 94 mins at 400 nL/min. Subsequent fractions were carried with increasing concentrations of solvent B. The following 4 first dimension fractions were eluted at 19.5, 22, 26, and 65% solvent B. The mass spectrometer was operated in positive data-dependent acquisition mode. MS1 spectra were measured with a resolution of 70,000, an AGC target of 1e6

and a mass range from 350 to 1700 m/z. Up to 12 MS2 spectra per duty cycle were triggered, fragmented by HCD, and acquired with a resolution of 17,500 and an AGC target of 5e4, an isolation window of 2.0 m/z and a normalized collision energy of 25. Dynamic exclusion was enabled with duration of 20 secs.

All mass spectra were analyzed with MaxQuant software version 1.5.5.1. MS/MS spectra were searched against the *Mus musculus* Uniprot protein sequence database (version July 2016) and GPM cRAP sequences (commonly known protein contaminants). Precursor mass tolerance was set to 20 ppm and 4.5 ppm for the first search where initial mass recalibration was completed and for the main search, respectively. Product ions were searched with a mass tolerance 0.5 Da. The maximum precursor ion charge state used for searching was 7. Carbamidomethylation of cysteines was searched as a fixed modification, while oxidation of methionines and acetylation of protein N-terminal were searched as variable modifications. Enzyme was set to trypsin in a specific mode and a maximum of two missed cleavages was allowed for searching. The target-decoy-based false discovery rate (FDR) filter for spectrum and protein identification was set to 1%. 2DLC-MS/MS analysis and data analysis were performed by Proteomics Shared Resource in Sanford Burnham Prebys Medical Discovery Institute.

Immunofluorescence

Hearts were isolated from mice, rinsed in phosphate buffered saline (PBS), immersed in cold isopentane, and embedded in optical cutting temperature (OCT) Tissue-Tek (Thermo Fisher Scientific, Waltham, MA) on dry ice as previously described (5). Sections (10 μm) were cut using a Leica CM 3050S cryostat (Leica Microsystems, Bannockburn, IL) and fixed in acetone at -20°C for 5 mins. After permeabilization with blocking buffer

(PBS containing 5% normal donkey serum, 1% BSA), sections were incubated overnight in blocking buffer in a humidified chamber at 4°C with the indicated antibodies (listed in Supplementary Table 1). Subsequently, sections were rinsed in washing buffer (PBS with 0.2% TX-100) and incubated for 2 hours at room temperature with fluorescently-conjugated secondary antibodies and 4',6-diamidino-2-phenylindole (DAPI) (1:500) diluted in blocking buffer. Slides were rinsed in wash buffer and mounted in mounting buffer (Dako). Confocal microscopy was performed using an oil-immersed 60X objective, with 1.35 numerical aperture, on an inverted microscope controlled by a DeltaVision system (Applied Precision, Washington, USA).

Measurement of sarcomere shortening and calcium transients in adult cardiomyocytes

Adult cardiomyocytes were isolated from CKO or control mice, loaded with Fura-2-AM (1.0 μM, 15 mins), washed twice, and continuously perfused with Tyrode solution maintained at 37°C. Simultaneous measurement of intracellular Ca^{2+} (6) and cell contractility was performed using a video-based sarcomere length-detection system (IonOptix, Milton, MA). Myocytes were field stimulated at a frequency of 0.5, 0.75, 1.0, 2.0, and 4.0 Hz using a pair of platinum wires placed on the opposite sides of the dish chamber and connected to a MyoPacer Field Stimulator (IonOptix). Typically 15–25 individual myocytes were recorded and analyzed for each heart. The ratio of Fura-2 fluorescence at 340 nm and 380 nm (R) was calculated and the amplitude of intracellular Ca^{2+} transient was determined by the change between the basal and peak ratio (ΔR). The amplitude of cell contraction was assessed by peak shortening, and the rate of cell relaxation was assessed by the time to 63% re-lengthening (Tau).

Induction and evaluation of autophagic flux

BAG3 CKO, cMUT, CKO$^{LC3\text{-}GFP}$ and control littermates were fasted for 24 hours to induce autophagy. The method of evaluating autophagic flux by using the ratio of LC3B-II to LC3-I in western blot and GFP-LC3 puncta has been described previously (7). Neonatal cardiomyocytes isolated from wildtype (WT) and BAG3 global knockout (KO) mice were treated with glucose-free serum-free DMEM medium (11966-025, Invitrogen) for 2 hours to obtain starvation conditions. Bafilomycin-A1 (100 nM) or Chloroquine (40 μM) was used for the inhibition of autophagosome-lysosome fusion and autophagosome degradation during starvation (8). Cells were lysed and the ratio of LC3B-II to LC3-I was assessed by western blot to evaluate the level of autophagic flux (9).

Supplemental figure legend

Figure S1. (Relative to Figure 1) BAG3 deficiency leads to DCM and premature death. (A) Targeting strategy for the generation of *BAG3* knockout mice. **(B)** Representative image to illustrate significant growth retardation in *BAG3* global knockout mice compared with wildtype (WT) littermates at 20 days of age (scale bar: 1 cm). **(C)** Kaplan-Meier survival curves of *BAG3* global knockout homozygous (-/-), heterozygous (+/-) and control (+/+) mice. n=10 mice per group. **(D)** Growth curves of BAG3 global knockout homozygous (-/-), heterozygous (+/-) and control (+/+) mice. n=10 mice per group. **(E)** qRT-PCR analysis of *BAG1*, *BAG2*, *BAG4*, *BAG5*, *BAG6* in control (Ctrl) (n=9) and $BAG3^{f/f}$; α-MHC-Cre positive (CKO) (n=8) mouse hearts at 4 months. Data is normalized to corresponding 18S levels. **(F-G)** Hemodynamic measurements of contractile function in Ctrl (n=7) and BAG3 CKO (n=11) mice in response to increasing levels of the beta 1 adrenergic agonist dobutamine at 10 weeks. **(H-I)** The contractility of adult cardiomyocytes isolated from Ctrl and BAG3 CKO mice were measured using a sarcomere length-detection system. The amplitude of cell contraction was assessed by peak shortening (H), and the rate of cell relaxation was assessed by the time to 63% re-lengthening (Tau) (I). **(J-K)** The amplitude (J) and Tau (K) of Ca^{2+} transients of Ctrl (blue) and BAG3 CKO (red) cardiomyocytes were measured at 0.5, 0.75, 1.0, 2.0, and 4.0 Hz, respectively. Data are represented as mean ± SEM; **P*<0.05 according to 2-tailed Student's t test.

Figure S2. Echocardiographic measurements from wildtype (WT) (n=5) and αMHC-Cre positive (Cre+) (n=6) mice at 10 months. (A) Left ventricle (LV) fractional

shortening (FS); **(B-C)** LV internal diameter at end diastole (B) LV internal diameter at and end systole (C). Data are represented as mean ± SEM.

Figure S3. BAG3 deficiency leads to protein instability of sHSPs. (A) qRT-PCR analysis of *HSPB8/6/5* in BAG3 global knockout (KO) (n=5) and wildtype (WT) control (n=4) hearts at 2 weeks. Data is normalized to corresponding 18S levels. **(B)** Western blot analysis of HSPB8 in neonatal cardiomyocytes isolated from WT control and BAG3 KO mice treated with cycloheximide (CHX, 10 μg/ml) for 24 hours. DMSO was used as a control. n=3. GAPDH served as a loading control. **(C-D)** Representative western blot (C) and quantification analysis (D) of overexpressed Dendra2-HSPB8 in neonatal cardiomyocytes isolated from WT control and BAG3 KO mice infected with HSPB8 fused with Dendra2 taq overexpressing adenovirus (20 MOI). After 24 hour infection, cardiomyocytes were treated with CHX (10 μg/ml) for 0, 3, 12, 18, 24 hours. GAPDH served as a loading control. Data are represented as mean ± SEM; **P*<0.05 according to 2-tailed Student's t test.

Figure S4. Autophagic flux is suppressed in BAG3 knockout hearts and cardiomyocytes. (A-B) Representative Western blot (A) and quantification analysis (B) of cardiac autophagic flux assessed by the ratio of LC3-II to LC3-I in control (Ctrl) and $BAG3^{f/f}$; αMHC-Cre positive (CKO) hearts after 18 hour fasting. n=4 mice per group. **(C-D)** Representative Western blot (C) and quantification analysis (D) of p62 protein levels in cardiac tissues from Ctrl and BAG3 CKO mice. n=4 mice per group. **(E-F)** Representative Western blot (E) and quantification analysis (F) for starvation-induced cardiac autophagic flux assessed by the ratio of LC3-II to LC3-I in neonatal cardiomyocytes isolated from wildtype (WT) control and BAG3 knockout (KO) mice. NR:

Nutrition rich; ST: starvation 3 hours in glucose and serum deplete medium. n=5. **(G-H)** Representative images (G) and quantification analysis (H) of cardiac tissue sections from Ctrl and BAG3 CKO mice crossed with GFP-LC3 (green) transgenic mice after 18 hour fasting. α-actinin and Nkx2.5 staining were used for labeling cardiomyocytes. n=4 mice per group. **(I-J)** Representative immunoblots (I) and quantification analysis (J) for cardiac autophagic flux assessed by the ratio of LC3-II to LC3-I in neonatal cardiomyocytes isolated from WT and BAG3 KO mice under different treatment conditions for 3 hours. GAPDH served as a loading control. NR: Nutrition rich; ST: starvation in glucose and serum deplete medium; BAF: Bafilomycin A1; Chl: Chloroquine. GAPDH was used as loading control. n=4. Data are represented as mean ± SEM; *P<0.05 according to 2-tailed Student's t test or two way ANOVA.

Figure S5. Immunofluorescence analysis of BAG3-related proteins (A) p62, **(B)** Desmin,and **(C)** αB-crystalin in myocardium of control (Ctrl) and $BAG3^{f/f}$; α-MHC-Cre positive (CKO) mice. n=3 mice per group. Scale bars: 5 μm.

Figure S6. Volcano Plot showing P values (-log10) versus protein quantitation ratio of CKO/Ctrl (log2) of total proteins from iTRAQ analysis of BAG3 CKO and control hearts.

Figure S7. (Relative to Figure 3) BAG3 deficiency leads to increased levels of a subset of insoluble proteins. (A) Western blot validation of mass spectrometry analysis of insoluble fraction proteins from Ctrl and CKO mouse hearts. n = 4. Loading control in Figure 3B was used for replicate samples in Figure 7A. **(B)** Network visualization of the highly differentially expressed proteins from insoluble fraction of Ctrl versus CKO mouse hearts. Red nodes represent increased proteins (fold change

greater than 3 in CKO/Ctrl). Blue nodes represent decreased proteins (fold change less than 0.5 in CKO/Ctrl). Enriched gene ontology (GO) terms of network modules were defined by DAVID functional annotation tool.

Figure S8. Localization of BAG3 in adult mouse heart. (A) BAG3 is present in both non-filament and filament fractions of total proteins isolated from wildtype adult mouse ventricles. Cypher is a known Z-disk protein. GAPDH was used as a cytosolic protein marker. **(B)** BAG3 is present in both cytoplasmic and mitochondrial fractions of total proteins isolated from wildtype adult mouse ventricles. VDAC2 and GAPDH were used as mitochondrial and cytosolic protein markers, respectively. **(C)** BAG3 (green) colocalizes with α-Actinin (red) at Z-disks (arrowheads) in wildtype mouse heart sections.

Figure S9. (Relative to Figure 6) E455 amino acid is critical for BAG3 function. (A) Targeting strategy for the generation of E455K knock-in mice. Neo, neomycin resistance gene; DTA, Diphtheria Toxin A chain gene. Green boxes abutted to the Neo gene indicate FRT sites. **(B)** Detection of wildtype (+) and mutant (m) alleles by Southern blot analysis. **(C)** Genotyping of *BAG3* E455K mutant mice. **(D)** Immunofluorescence analysis of BAG3 in myocardium of control (Ctrl) and cardiac-specific BAG3 E455K mutant (cMUT) mice. Scale bars: 2 μm. n=3 mice per group. **(E)** Representative Western blot analysis of HSP90, HSP70, HSC70 in cardiac tissues from Ctrl and cMUT mice. n=4 mice per group. **(F)** Representative Western blot analysis of cardiac autophagic flux assessed by the ratio of LC3B-II to LC3B-I in Ctrl and cMUT hearts after 18 hour fasting. GAPDH served as a loading control. n=4 mice per group.

Figure S10. Echocardiographic measurements from cardiac specific BAG3 E455K mutant (cMUT) and control (Ctrl) mice at 6 months. (A) Representative images of

echocardiography from Ctrl and cMUT mice at 6 months. **(B-D)** Echocardiographic measurements from Ctrl (n=9) and cMUT (n=8) mice at 6 months of (B) left ventricle (LV) fractional shortening (FS), (C) LV internal diameter at end diastole and (D) LV internal diameter at end systole. Data are represented as mean ± SEM; *P<0.05 according to 2-tailed Student's t test.

Supplemental table 1. 39 of potential BAG3 binding partners were overlapping with proteins increased in the insoluble protein fraction from BAG3 CKO hearts.

Protein names	CKO/WT (insoluble protein fraction)	Protein names	CKO/WT (insoluble protein fraction)
Heat shock 70 kDa protein 1A;Heat shock 70 kDa protein 1B	3.63	Cytochrome c oxidase subunit NDUFA4	1.53
Stress-70 protein, mitochondrial	2.71	Carnitine O-palmitoyltransferase 1, muscle isoform	1.69
Alpha-crystallin B chain	4.63	Voltage-dependent anion-selective channel protein 2	5.14
Heat shock protein beta-1	2.85	Apoptosis-inducing factor 1, mitochondrial	4.64
Heat shock protein beta-7	3.69	Calcium-binding mitochondrial carrier protein Aralar2	1.97
DnaJ homolog subfamily C member 11	2.48	Cytochrome c oxidase subunit 2	2.15
60S ribosomal protein L27	2.12	Acetyl-CoA acetyltransferase, mitochondrial	4.25
60S ribosomal protein L7	2.07	ATP synthase-coupling factor 6, mitochondrial	4.31
60S ribosomal protein L21	1.86	Microtubule-associated protein 4	3.02
60S ribosomal protein L36	3.24	Syntenin-1	5.46
60S ribosomal protein L8	2.33	EH domain-containing protein 2	1.97
60S ribosomal protein L4	2.19	Nascent polypeptide-associated complex subunit alpha, muscle-specific form	2.53
60S ribosomal protein L6	1.71	Rab11 family-interacting protein 5	11.07
Proteasome subunit alpha type-5	6.19	Sorbin and SH3 domain-containing protein 2	1.95
LIM domain-binding protein 3	1.86	A-kinase anchor protein 2	2.48
Nebulette	1.85	Synaptopodin	2.47
Myosin-binding protein C, cardiac-type	2.27	KN motif and ankyrin repeat domain-containing protein 2	2.06
Calsequestrin-2	2.23	Ragulator complex protein LAMTOR1	3.48
PDZ and LIM domain protein 5	1.65	Type 2 phosphatidylinositol 4,5-bisphosphate 4-phosphatase	5.55
Filamin-C	4.24		

Supplemental table 2. Antibody list

Antibody	Source, Cat. No	Antibody	Source, Cat. No
α-actinin	Sigma-Aldrich, A7811	HSPB7	Abcam, ab150390
α-Tropomyosin	Abcam, ab133292	LAMTOR	Cell signaling, #8975
αB-crystallin/ HSPB5	Enzo Life Sciences, ADI-SPA-223	LC3B	Cell Signaling, 2775S
ACAT1	Novus biologicals, NBP1-89285	MAP4	Bethyl, A301-489A
BAG3	Proteintech, 10599-1-AP	MTCO2/COX2	Santa cruz, sc-1745
CapZβ	Santa cruz, sc-136502	MYBPC3	Santa cruz, sc-50115
Cypher	1495 as previously described(10)	pan-Myosin Heavey Chain/ MyHC	DSHB, MF20
Desmin	Santa cruz, sc-7559	Myozenin	Sigma-Aldrich, HPA037848
Filamin C	Santa cruz, sc-48496	Naca-rs	Abcam, ab171018
ENH	Abnova, H00010611-A02	FIS1	Proteintech, 10956-1-AP
HADHB	Abcam, ab110302	UQCRB	Abcam, EPR15591
HSC70/HSP73	Enzo Life Sciences, ADI-SPA-815-F	OXPHOS cocktail	Abcam, ab110413
Flag	Sigma-Aldrich, F3165	PSMA5	Bethyl, A302-749A-T
GAPDH	Santa cruz, sc-32233	SQSTM1/p62	PROGEN Biotechnik, GP62-C
HSP20/HSPB6	R&D, MAB4200	HSP90	Abcam, ab178854
HSP22/ HSPB8	Abcam ab151552 or provide by Hongyu Qiu(11)	VDAC2	Abcam, ab37985
HSP70/HSP72	Enzo Life Sciences, ADI-SPA-810-D	Vinculin	Sigma-Aldrich, V9131

Supplemental table 3. Primer list

Primer for qRT-PCR:		
Gene	**Forward**	**Reverse**
BAG1	GCAGCAGGGAGTTGACTAGAA	TTACTTCCTCGGTTTGGGTCG
BAG2	AGACGCAGCTACTGCTGTTG	CGGATCGTTTCCACCGAGAC
BAG4	AGTGACGGCCCTTCTTACG	CCGAGGGGTAGTAGCCATC
BAG5	GGAAGCTGACAGTACACATGC	GCGCCTGGAGAAGTTCATTTT
BAG6	CAACAGCACCAACTCGGGT	TCTGGGCCAATGAAGTGTTTG
ANF	GATAGATGAAGGCAGGAAGCCGC	AGGATTGGAGCCCAGAGTGGACTAGG
BNP	TGTTTCTGCTTTTCCTTTATCTGTC	CTCCGACTTTTCTCTTATCAGCTC
Collagen 1a1	TCACCAAACTCAGAAGATGTAGGA	GACCAGGAGGACCAGGAAG
Collagen 3a1	ACAGCAGTCCAACGTAGATGAAT	TCACAGATTATGTCATCGCAAAG
HSPB8	TCCCGTGCTCCTACCCAAG	GCTGTCAAGTCGTCTGGAAAAG
HSPB6	GCCCGGATGAACACGGATT	CAGGTGGTGACGGAAGTTGG
HSPB5	GTTCTTCGGAGAGCACCTGTT	GAGAGTCCGGTGTCAATCCAG
18S	GGAAGGGCACCACCAGGAGT	TGCAGCCCCGGACATCTAAG
Primer for genotyping:		
BAG3 wildtype allele:	ATCAGCATAGCACAGCTGGA	GGATCAAGAGAATGCCTGGT
BAG3 Knockout allele:	ACCATTACCAGTTGGTCTGG	GGATCAAGAGAATGCCTGGT
BAG3 floxed allele:	TGGTTTGCCACTATCTGCTG	GCACACCAAGGAGTCAAAGT
E455K mutant allele:	TCCTTGTCTGTAAGGCTGTCAC	CAACCTGCAGAGATTTCTACCC
αMHC-Cre:	GCCATAGGCTACGGTGTAAAAG	ATAATCGCGAACATCTTCAGGT

Supplemental references

1. Ayyadevara S, Mercanti F, Wang X, Mackintosh SG, Tackett AJ, Prayaga SV, Romeo F, Shmookler Reis RJ, and Mehta JL. Age- and Hypertension-Associated Protein Aggregates in Mouse Heart Have Similar Proteomic Profiles. *Hypertension.* 2016;67(5):1006-13.
2. Wu G, Feng X, and Stein L. A human functional protein interaction network and its application to cancer data analysis. *Genome Biol.* 2010;11(5):R53.
3. Shannon P, Markiel A, Ozier O, Baliga NS, Wang JT, Ramage D, Amin N, Schwikowski B, and Ideker T. Cytoscape: a software environment for integrated models of biomolecular interaction networks. *Genome Res.* 2003;13(11):2498-504.
4. Chen J, Bardes EE, Aronow BJ, and Jegga AG. ToppGene Suite for gene list enrichment analysis and candidate gene prioritization. *Nucleic Acids Res.* 2009;37(Web Server issue):W305-11.
5. Boogerd CJ, Aneas I, Sakabe N, Dirschinger RJ, Cheng QJ, Zhou B, Chen J, Nobrega MA, and Evans SM. Probing chromatin landscape reveals roles of endocardial TBX20 in septation. *J Clin Invest.* 2016;126(8):3023-35.
6. Pereira L, Cheng H, Lao DH, Na L, van Oort RJ, Brown JH, Wehrens XH, Chen J, and Bers DM. Epac2 mediates cardiac beta1-adrenergic-dependent sarcoplasmic reticulum Ca2+ leak and arrhythmia. *Circulation.* 2013;127(8):913-22.
7. Mizushima N. Methods for monitoring autophagy using GFP-LC3 transgenic mice. *Methods in enzymology.* 2009;452(13-23.
8. Kim YC, Park HW, Sciarretta S, Mo JS, Jewell JL, Russell RC, Wu X, Sadoshima J, and Guan KL. Rag GTPases are cardioprotective by regulating lysosomal function. *Nature communications.* 2014;5(4241.
9. Sciarretta S, Zhai P, Shao D, Zablocki D, Nagarajan N, Terada LS, Volpe M, and Sadoshima J. Activation of NADPH oxidase 4 in the endoplasmic reticulum promotes cardiomyocyte autophagy and survival during energy stress through the protein kinase RNA-activated-like endoplasmic reticulum kinase/eukaryotic initiation factor 2alpha/activating transcription factor 4 pathway. *Circulation research.* 2013;113(11):1253-64.
10. Huang C, Zhou Q, Liang P, Hollander MS, Sheikh F, Li X, Greaser M, Shelton GD, Evans S, and Chen J. Characterization and in vivo functional analysis of splice variants of cypher. *The Journal of biological chemistry.* 2003;278(9):7360-5.
11. Qiu H, Lizano P, Laure L, Sui X, Rashed E, Park JY, Hong C, Gao S, Holle E, Morin D, et al. H11 kinase/heat shock protein 22 deletion impairs both nuclear and mitochondrial functions of STAT3 and accelerates the transition into heart failure on cardiac overload. *Circulation.* 2011;124(4):406-15.